Journal of Civil & Environmental Engineering

Abdrabbo et al., J Civil Environ Eng 2016, 6:2
DOI: 10.4172/2165-784X.1000216

Research Article | Open Access

The Effect of Water Mist Droplet Size and Nozzle Flow Rate on Fire Extinction in Hanger by Using FDS

Mohamed Fayek Abdrabbo[2], Ayoub Mostafa Ayoub[3], Mohamed Aly Ibrahim[1] and Abdelsalam M. Shara Feldin[1]*

[1]*Benha University, Faculty of Engineering, Shoubra, Egypt*
[2]*Egyptian University for Administration Science and Technology, Cairo, Egypt*
[3]*October 6 University, 6th of October city, Giza, Egypt*

Abstract

Water is playing a vital role and widely used in our life. The use of water for fire extinction and extinguishment is widespread because of the following reasons. The first is economic. A second reason is that many fire safety. Fire suppression by using water mist is widely considered to be an alternative to gaseous fire suppression agents. A lot of commercial activity has occurred in the last years to develop technology for fire suppression systems based on water mist. The objective of this paper is to investigate the effectiveness of water mist with various droplet sizes and various nozzle flow rate on fire suppression in hanger, taking into account extinguishing time, gas concentration, and temperature decay. Three nozzle flow rate with the same conditions were employed and different droplet size provided. It was found that the extinguishing time decreases with the droplet size decrease and flow rate increase. The temperature decay rate was improved by decreasing the droplet diameter or increasing the flow rate. In addition, with an increase in the extinguishing time, the concentration of O_2 decreased while CO_2 increased. The study is carried out using Fire dynamic simulator (FDS) combined with PYROSIM and SMOKEVIEW programs. These programs, to achieve the model of compartment fire scenario require investigating and determining temperature and gas concentration.

Keywords: Droplet; FDS; Fire Extinction; Nozzle flow; Water mist

Introduction

The use of very fine water sprays to extinguish fires has received much renewed attention in the last years. It is of some advantages such as [1,2].

1. Replacement for halon and CO_2 systems in many applications.
2. Safer than CO_2.
3. Cools the fire area dramatically.
4. Uses less water than conventional sprinklers
5. Prevents reignition.
6. Has some smoke scrubbing qualities.
7. Can be used to suppress explosions.

It is acknowledged that the spray cone angle and flow rate of nozzle play a vital role in fire suppression performance, as well as cover area and water consumption. However, few studies have been done on the relationship between above parameters. Many researchers have studied the fire suppression by using water mist in compartment. Chuka et al**.**, [2] studied the effects of the droplet size and injection orientation on water mist suppression of liquid pool fires. The base injection of droplets enhanced the suppression effectiveness by as much as two times compared to top injection, and small droplets were more effective in every orientation. Liu Yinshui et al., [3] studied an experimental study of the effectiveness of fire suppression performance by changing characteristics of nozzles. They used two groups of pressure-swirl nozzles with the same flow rate and different spray cone angles were employed. They concluded that the angle was adjusted by changing diameters and lengths of entrance, swirl chamber and orifice of nozzle. It was found that the cover area and the droplet size increased slightly with the spray angle. The fire tests results showed that the extinguishing time increased with the spray cone angle, and increased with the flow rate and the operating pressure decreasing. Sung et al. [4] conducted experiments using pool fire with a water mist nozzles positioned directly above it, and also did the parallel scenario simulations. On the contrary, he discovered that the introduction of water mist increased the fire Heat Release (HRR) Rate measurements which he attributed to air entrainment from the mist providing increased turbulence mixing between oxygen and fuel vapours. Expanding on this theory, he introduced the concept of increasing the HRR in the simulation after water mist activation which resulted in his simulations closely representing the experimental results. Further tests showed that HRR increased with water flow rate and decreased as fire size increased. The flaw in this concept is that this increase in HRR would vary with different scenarios; therefore experiments have to be done before simulations which defeat the purpose of simulation predictions. He found that if the spray momentum was greater than the plume buoyancy, the main extinguishing mechanism was gas phase cooling as water could penetrate into the flame region. Otherwise, oxygen depletion was the main contributing factor for extinguishment. Benjamin Piers Hume [5] studied a new type of water mist system where by air and water mist are blown into a fire compartment at low level using a displacement ventilation system. He investigated the feasibility of this concept a test compartment and associated displacement water mist system were designed based in the standard ISO room. A full-scale test compartment was built and tests run for a number of 20 kW fires of different types and in different positions. The basic setup and a selection of fires were also simulated using the computational fluid dynamics program Fire Dynamics Simulator (FDS). Gerard et al., [6] studied the performance of nozzles, e.g. flow rate, spray cone angle,

***Corresponding author:** Abdelsalam M. Shara Feldin, Benha University, Shoubra, Egypt, Tel: +20 13 3231011; E-mail: a.sharafeldin84@gmail.com

Received January 13, 2016; **Accepted** February 10, 2016; **Published** February 12, 2016

Citation: Abdrabbo MF, Ayoub AM, Ibrahim MA, Feldin AMS (2016) The Effect of Water Mist Droplet Size and Nozzle Flow Rate on Fire Extinction in Hanger by Using FDS. J Civil Environ Eng 6: 216. doi:10.4172/2165-784X.1000216

size and distribution of droplet, and discharging direction, have a great effect on fire suppression. Fire Suppression tests with different flow rates, fire sizes, and vent areas. He found that the flux density reduced the compartment temperature but had little effect on the oxygen concentrations in the compartment. Hua et al., [7] used a numerical model to investigate the influence of nozzle characteristics on fire suppression. The monodisperse spray was treated using a Lagrangian's approach. They concluded that a water spray with a solid cone pattern and a finer water droplet is more efficient in suppressing fires than a hollow cone pattern and a coarser water size. The research explore the possibility of using the computational fluid dynamics program FDS (Fire Dynamics Simulator) as a computational design. FDS is widely used in fire engineering design and thus it is important that the capabilities of the program for modeling this problem are known. FDS has been used for various applications including modeling smoke flow in multi-floors buildings, tunnel fires and different ventilation conditions.

FDS Model Description

The dimensions of the FDS model hanger (inclined surface) and the burner dimensions and its position in compartment are 4 m × 6 m × 3.75 m (length × width × height) and a door opening is located at the front of the compartment. The fire is modeled with a cubic heat source, the fire source has dimension of 0.5 m × 1m × 0.4 m (length x width x height), (Figure 1). A six water mist nozzle is used in the model. The nozzle specifications are indicated in Table 1 the fuel is used in the simulation is Methane. The fire takes place at the end of compartment (in the corner).The door in all cases are taken to be fully opened, as given in Figure 1. The input file for each simulation is generated for the same model, with water mist nozzle specifications as shown in Table 1.

Grid Resolution

A 0.1 m grid is specified for the hanger, with a total of 96480 cells respectively. This simulation took around 48 hours each to run. The selection of mesh size get from FDS User Guide [8], it states to use a

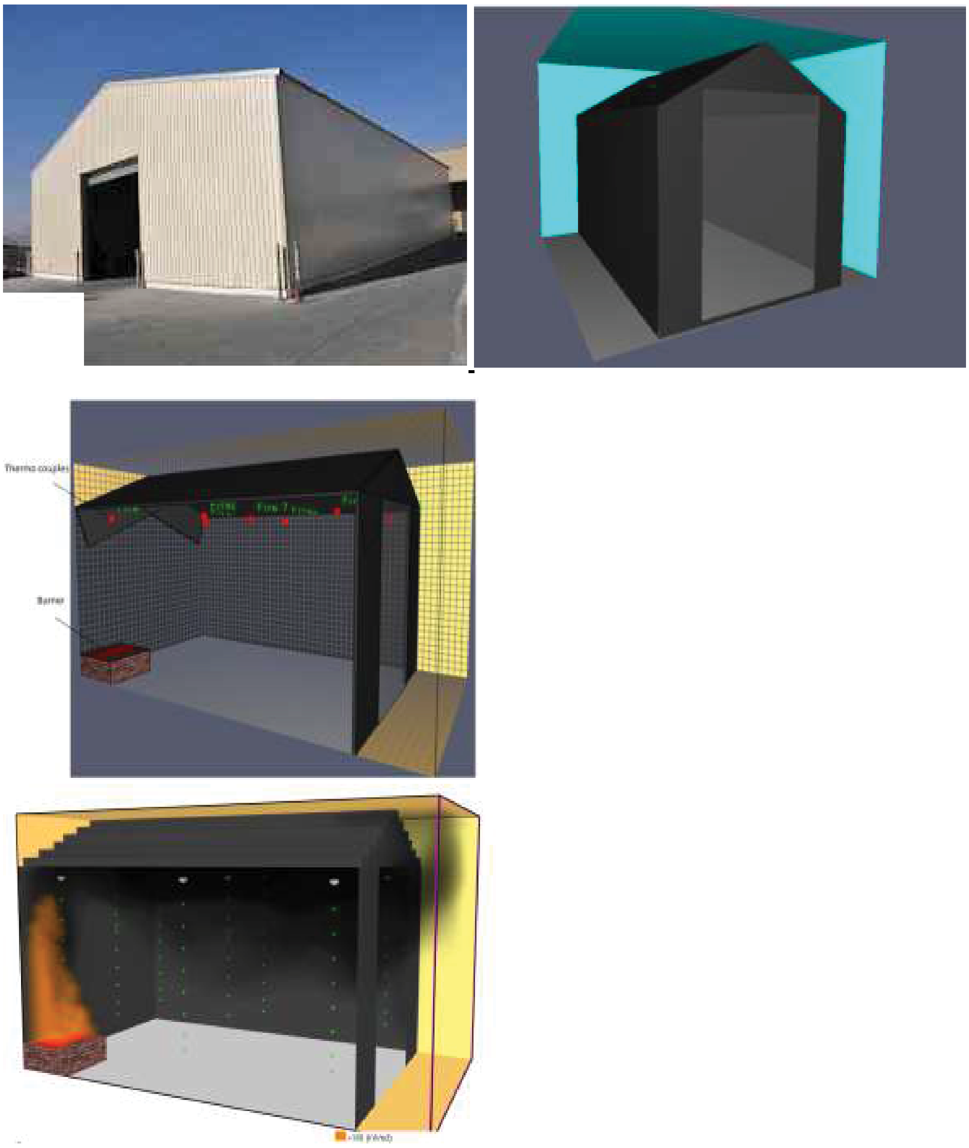

Figure 1: Fire compartment model (pyrosim).

Citation: Abdrabbo MF, Ayoub AM, Ibrahim MA, Feldin AMS (2016) The Effect of Water Mist Droplet Size and Nozzle Flow Rate on Fire Extinction in Hanger by Using FDS. J Civil Environ Eng 6: 216. doi:10.4172/2165-784X.1000216

Diameter	121 μm
Orifice diameter	3 mm
Operating pressure	13 bar
Flow rate	25-50 L/m
K- factor	3.6
Spray angle	60,90 and 120°

Table 1: The spray specifications of nozzle.

D*/dx ratio between 4 and 16 in order to determine the appropriate mesh size. In that ratio, dx is the nominal size of a mesh cell, and D* is a characteristic fire diameter defined in the following equation:

$$D^* = \left(\frac{\dot{Q}}{\rho_\infty * C_p * T_\infty * \sqrt{g}} \right)^{2/5} \tag{1}$$

Where Q is the heat release rate; ρ_∞ is the density of air (1.204 kg/m^3); C_p is the specific heat of air(1.005 kJ/kg.K); T_∞ is the ambient temperature(293 K); and g is the acceleration due to gravity(9.81 m/s^2). The finest mesh size we would have to use is with a D*/dx ratio of 16.

Grid Independency Check

The stability and the robust of the grid should be tested.This could attain through comparisons of the same case but for different grid sizes (Table 2). Three different mesh sizes are used to simulate one case in addition to finer grid. The comparisons is made measure average temperatures for fire spread without misting with heat release rate 1000 kW/m^2 for hanger. The average mist flux for normal room with misting are measured with four different mesh sizes.

A 0.1 m is used, because of moderate mesh size and could not take much simulation run times. A 0.01 m grid could not be used due to the extensive simulation run times required (Figure 2).

Governing Equations

This section introduces the basic conservation equations for mass, momentum and energy for a Newtonian fluid. These are the same equations that can be found in almost any textbook on fluid dynamics or CFD. A particularly useful reference for a description of the equations, the notation used, and the various approximations employed is Anderson et al., [9] noted that this is a set of partial differential equations consisting of six equations for six unknowns, all functions of three spatial dimensions and time: the density ρ, the three components of velocity u = [u; v; w]T, the temperature T, and the pressure p.

The continuity equation can be simplified as the following relation:

$$\frac{\partial \rho}{\partial t} + \frac{\partial(\rho u)}{\partial x} + \frac{\partial(\rho v)}{\partial y} + \frac{\partial(\rho w)}{\partial z} = 0 \tag{2}$$

When the flow is at steady –state, ρ does not change with respect

time. The continuity equation is reduced to:

$$\frac{\partial(\rho u)}{\partial x} + \frac{\partial(\rho v)}{\partial y} + \frac{\partial(\rho w)}{\partial z} = 0 \tag{3}$$

The momentum equations with the velocity components (the dependent variables to be solved for) are typically named u, v , w. while the three equations are:

$$\rho\left(\frac{\partial u}{\partial t} + u\frac{\partial u}{\partial x} + \upsilon\frac{\partial u}{\partial y} + w\frac{\partial u}{\partial z}\right) = -\frac{\partial p}{\partial x} + \mu\left(\frac{\partial^2 u}{\partial x^2} + \frac{\partial^2 u}{\partial y^2} + \frac{\partial^2 u}{\partial z^2}\right) + \rho g_x \tag{4}$$

$$\rho\left(\frac{\partial u}{\partial t} + u\frac{\partial u}{\partial x} + \upsilon\frac{\partial u}{\partial y} + w\frac{\partial u}{\partial z}\right) = -\frac{\partial p}{\partial y} + \mu\left(\frac{\partial^2 u}{\partial x^2} + \frac{\partial^2 u}{\partial y^2} + \frac{\partial^2 u}{\partial z^2}\right) + \rho g_y \tag{5}$$

Grid	Mesh size (m)	Cell numbers
I	0.08	189000
II	0.10	96480
III	0.16	23400

Table 2: Different mesh size (hanger).

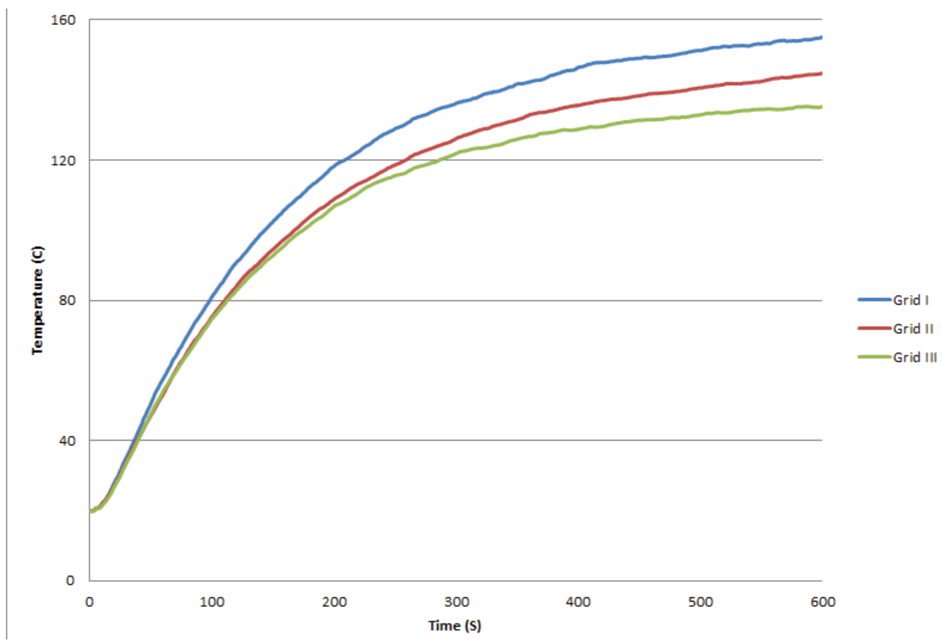

Figure 2: Average temperature measurements with time.

$$\rho\left(\frac{\partial u}{\partial t}+u\frac{\partial u}{\partial x}+\upsilon\frac{\partial u}{\partial y}+w\frac{\partial u}{\partial z}\right)=-\frac{\partial p}{\partial z}+\mu\left(\frac{\partial^2 u}{\partial x^2}+\frac{\partial^2 u}{\partial y^2}+\frac{\partial^2 u}{\partial z^2}\right)+\rho g_z \quad (6)$$

Note that gravity has been accounted for as a body force, and the values of gx, gy, gz will be depend on the orientation of gravity with respect to the chosen set of coordinates. The energy equation in a multi-component reacting system, there are several mechanisms that contribute to the total heat flux, the most common known as conduction, convection and radiation. Mainly two additional effects are encountered in the literature; these are the effect of mechanical work done on the system due to buoyancy and the so-called Dufor effect. The latter describes the heat flux in a system due to concentration gradients and in general, this term can be neglected due to the low velocities involved in a fire the mechanical work term can be ignored as well. The energy equation can be written in different ways depending on which quantity is used as the dependent variable. Using the total enthalpy, $h_{total} = c_p T+\Sigma Y_\alpha H_r$ where H_r is the component heat of reaction, as dependent variable, the conservation of energy equation becomes:

$$\frac{\partial}{\partial T}(\rho H)+\frac{\partial}{\partial Xj}(\rho vjH)=\frac{\partial p}{\partial T}+\frac{\partial}{\partial Xj}\left[\frac{\lambda}{Cp}\frac{\partial h}{\partial Xj}-\dot{q}_j^r\right] \quad (7)$$

The program goes deeply in calculating all species quantities using complicated equation which will be very easy to be solved now a days by PC's other than manual old method. The program relations and equations can be found on site in a PDF file [8] for more details.

Temperature Measurement

The output quantity thermocouple is the temperature of a modelled thermocouple. The thermocouple temperature lags the true gas temperature by an amount determined mainly by its bead size. It is found by solving the following equation for the thermocouple temperature (T_{TC}),

$$\rho_{TC}c_{TC}\frac{dT_{TC}}{dt}=\varepsilon_{TC}(U/4-\sigma T_{TC}^4)+h_c(T_g-T_{TC})=0 \quad (8)$$

Where ε_{TC} the emissivity of the thermocouple, U is the integrated radiative intensity, T_g is the true gas temperature, and h is the heat transfer coefficient to a small sphere,

$h_c = kNu/d_{TC}$ The bead BEAD_DIAMETER, BEAD_EMISSIVITY, BEAD_DENSITY, and BEAD_SPECIFIC_HEAT are given on the associated PROP line. The default value for the bead diameter is 0.001 m. The default emissivity is 0.85. The default values for the bead density and specific heat are that of nickel; 8908 kg/m^3 and 0.44 kJ/kg/K, respectively. See the discussion on heat transfer to a water droplet in the Technical Reference Guide for details of the convective heat transfer to a small sphere.

Mixture Fraction Combustion Model

The mixture fraction representing the chemical reaction satisfies the conservation equation [10],

$$\rho\frac{DZ}{Dt}=\nabla.\rho D\nabla Z \quad (9)$$

If it is assumed that combustion occurs so rapidly that the oxygen and fuel cannot coexist, then both simultaneously vanish at a flame surface. This leads to a state relation between the oxygen mass fractions Y_O and the mixture fraction *Z*. Once, the mixture fraction at each location of domain computation is calculated in LES, the corresponding species concentration is obtained by reading from look-up table pre-defined [11]. The heat release rate is calculated from the mass consumption rate and the heat of combustion of the fuel as follows:

$$\dot{q}^m=\dot{m}_F^m\Delta H_F \quad (10)$$

Water Mist Droplet Models

The mechanisms of energy transfer between the fire and the water mist are the surface tension energy necessary to break-up the droplets, momentum to accelerate the droplets due to the velocity of the ambient gases, and energy to increase the temperature of the droplets due to the ambient temperature and the latent heat energy. Meanwhile, it is assumed in our work that the collisions between water mist droplets are negligible because the water mist spray seems to be relatively sparse [11].

Vaporization Model

The mass and energy transfer between the gas and the liquid droplets can be considered as follows [12]:

$$\frac{dm_l}{dt}=-A\,h_m\rho(Y_l-Y_g) \quad (11)$$

$$m_l c_l\frac{dT_l}{dt}=A\,h(T_g-T_l)+\dot{q}_r+\frac{dm_l}{dt}h_v \quad (12)$$

where, m_l is the mass of the liquid droplet, A is the surface area of the liquid droplet, h_m is the mass transfer coefficient to be discussed below, ρ is the gas density, c_l is the liquid specific heat, h is the heat transfer coefficient between the liquid and the gas, $\dot{q}_r$ is the rate of radiative heating of the droplet, and h_v is the latent heat of vaporization of the liquid, normally water. In mass transfer equation (7), Y_g is the vapor mass fraction of the gas obtained from the gas phase mass conservation equations and Y_l is the liquid equilibrium vapor mass fraction obtained from the Clausius-Clapeyron equation [10]. Mass and heat transfer between liquid and gas are described with analogous empirical correlations. The mass transfer coefficient, h_m and h heat transfer coefficients are described by the empirical relationships [12].

$$h_m=\frac{ShD_{lg}}{L} \quad (13)$$

$$h=\frac{Nu.k}{L} \quad (14)$$

Here, D_{lg} is the mass diffusion coefficient of water vapor in gas mixture; *L* is a length scale equal to the droplet diameter. *k* is the thermal conductivity of the gas. The Sherwood number Sh is evaluated from the Ranz and Marshall correlation [13] as follows:

$$Sh=2+0.6\,\mathrm{Re}_D^{0.5}\,Sc^{\frac{1}{3}} \quad (15)$$

Re_D is the Reynolds number of the droplet (based on the diameter, D, and the relative air-droplet velocity).

The Nusselt number Nu is evaluated with an analogous relationship as Sherwood number Sh,

$$Nu=2+0.6\,\mathrm{Re}_D^{0.5}\,\mathrm{Pr}^{\frac{1}{3}} \quad (16)$$

Pr is the Prandtl number (assumed 0.7 for all cases).

Model Accuracy

The desired accuracy for each predicted quantity depends on the technical issues associated with the analysis. You must ask the question: How accurate does the analysis have to be to answer the technical question posed? Returning to the earlier definitions of "design" and "reconstruction," design applications typically are more accurate because the heat release rate is typically specified rather than predicted, and the initial and boundary conditions are better characterized – at least in the analysis. Mathematically, a design calculation is an example of a "well-posed" problem in which the solution of the governing equations is advanced in time starting from a known set of initial conditions and constrained by a known set of boundary conditions. The accuracy of the results is a function of the fidelity of the numerical solution, which is mainly dependent on the size of the computational grid.

Specified Output

The following quantities are specified to be recorded in output files from the standard output generated by FDS can be seen in figures:

α) The grid of thermocouples is specified vertically and horizontally equally spaced 0.2 m.

β) Vertical slice files of the temperature, oxygen, carbon dioxide, carbon monoxide and fuel are recorded through the center of the window. A cross-sectional vertical slice of these quantities is also taken at mid-length of the compartment.

χ) The total mass flow and heat flow out of the window and the heat release rate within the compartment are recorded in CSV files, as are the total heat released and all thermocouple measurements.

δ) Oxygen volume fraction in the compartment also water vapour and carbon dioxide.

Note: all measurements output has taken at the center of compartment.

Results and Discussion

Effect of droplet size of water mist

Application of water in smaller droplets diameters offers several advantages [14]. Water mist droplet has small size, large surface area. The surface heat transfer coefficient has large value. When the ambient temperature rises, can quickly vaporize. Numerous small water droplets absorb heat rapidly in a short time. From the laws of thermodynamics: when one gram of water increases by 1°C, 1 card heat would be absorbed in this progress; when 1 gram of water vaporizes, about 600 calories would be absorbed. So, the role of vaporization of water mist fire can quickly reduce temperature. Meanwhile, the inerting effect of water mist like the physical effect of physical gas fire extinguishing, could reduce the oxygen concentration. In addition, water mist has a very excellent blocking performance of thermal radiation transfer, can effectively block the intense heat radiation. In this section the droplet sizes chosen are ranged from f 50, 350, 750 and 1000 µm. A water mist is actuated at 150 s after the fire ignition. Discharged from the nozzle, mists would suppress the fire by the direct cooling, the evaporation cooling, or the O_2 displacement. The temperature of hot gas layer is drastically cooled down after the activation of a water mist due to the evaporation heat removal from the mists. After the fire is extinguished by the mists, the hanger temperature would decrease gradually. Under the same conditions, simulations are conducted to investigate the fire extinguishing mechanisms for a water mist with different sizes of water droplets. Smaller droplets discharged from a water mist would be evaporated. This phenomenon causes the cooling of surrounding gas and the reduction of O_2 concentration due to the large amount of steam generation. Lack of sufficient O_2 and high temperature, the fire would be suppressed. With the relatively higher specific surface, smaller droplets would result in better heat transfer and more rapid vaporization. Therefore, the water mist with finer droplet sizes has the better performance of fire suppression. It is also shown in this figure that the performance of fire suppression slightly decreases with the increasing the droplet size, as its size. This calculated result is mainly obtained under the simulation assumption of same water injection flow rate. The number of droplets would be substantially reduced as their sizes increase under the same flow rate condition, which may decrease the capability of fire suppression. Figure 3 shows the average temperature for a water mist with the droplet sizes of 50, 350, 750 and 1000 µm

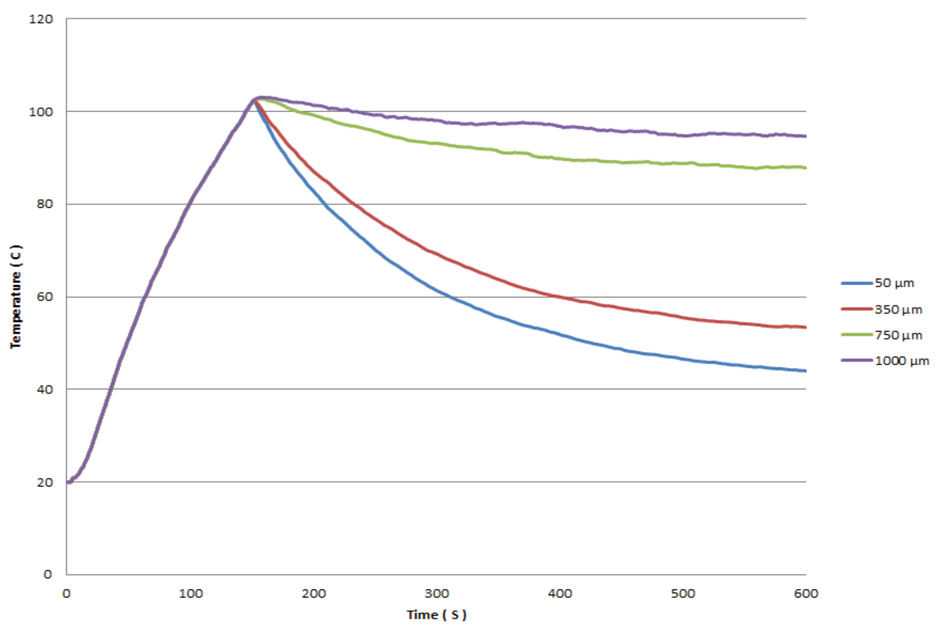

Figure 3: Average temperature with different droplet size.

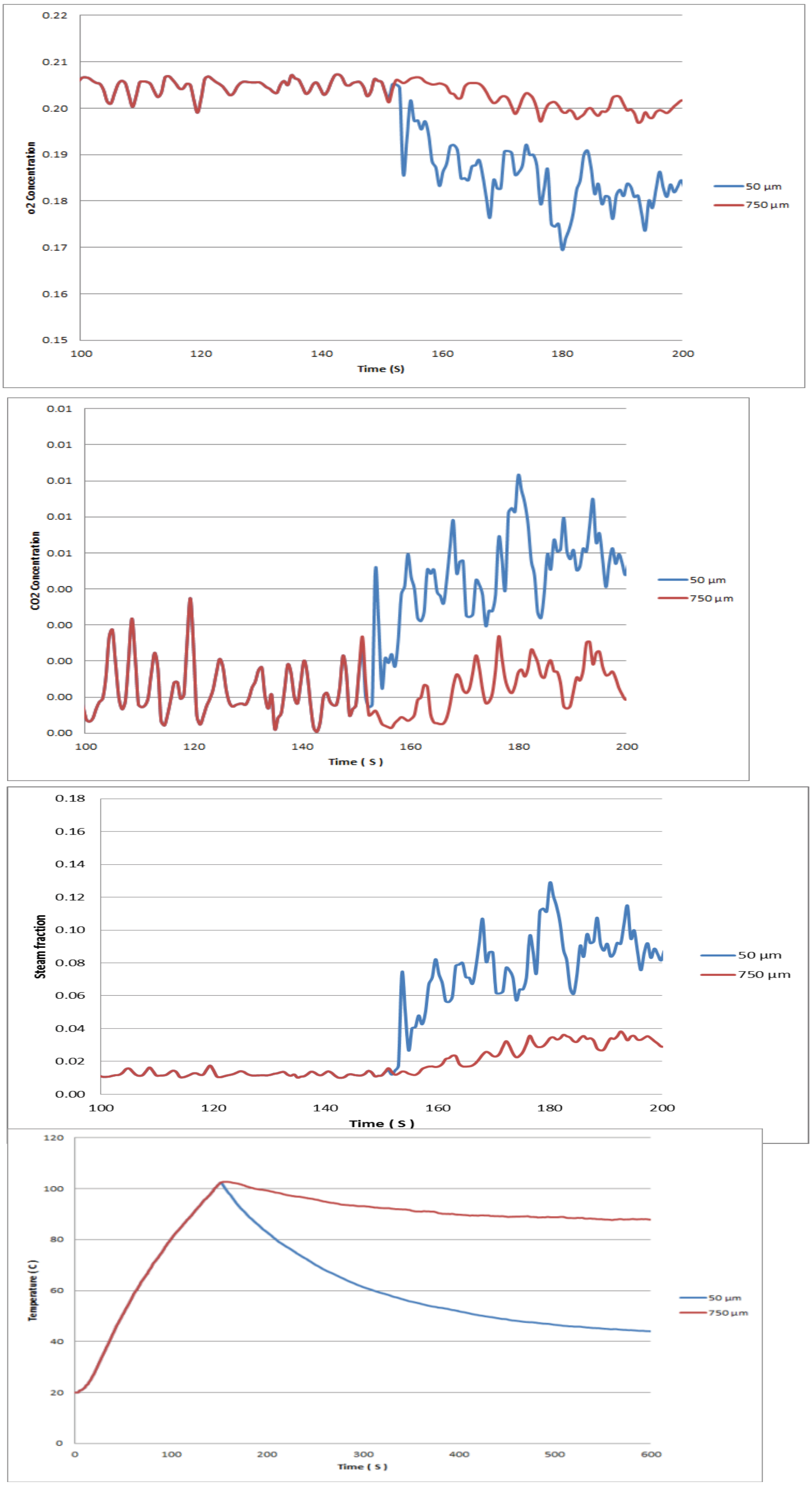

Figure 4: Temperature and gas concentration with droplet size 50 μm and 750 μm.

respectively. As discussed above, the fire is essentially extinguished by the droplet evaporation and the O_2 displacement for a water mist with smaller-size droplets. There-fore, just before the fire extinguishment, the temperature is close to the saturated temperature (100ºC). Figure 4 shows the corresponding time histories of steam fraction, O_2 and CO_2 concentrations for droplet sizes 50 and 750 µm also confirm it. The O_2 concentration for a water mist with the smaller-size droplet (50 µm) is reduced, which cannot sustain a fire. However, the corresponding O_2 concentration for the larger-size droplet (750 µm) is still kept. These calculated results indicate that the droplet evaporation is essentially the dominant mechanism of fire suppression for a water mist with relatively small-size droplets. As the aforementioned description, the O_2 displacement is the main mechanism to suppress a fire for a water mist with smaller size droplets. Figures 5-10 shows the shaded contours of steam fraction, O_2 and Temperature for a water mist with the droplet size of 50 µm and 750 µm after the spray activation. These plots are presented by cutting the central plane of solution domain and different locations of hanger. As a water mist discharges the droplets of 50 µm, most of droplets are quickly evaporated due to high temperature from the fire, consequently causing the sudden increase in the steam fraction along the trajectory of droplet flow. Enough steam generated from the droplet evaporation surrounds the fire. In the meantime, the generated steam would displace the rest of gases including O_2, causing a great reduction in the O_2 concentration. Also contours confirmed that the droplet size of 50 µm better than 750 µm for fire suppression as discussed before.

Effect of nozzle flow rate

Figure 11 shows the average temperature with fire extinguishment time using the spray nozzles with three different flow rate (5, 25 and 100) L/min. In this figure, at 150 s after the water injection the water droplets begin to spray downward and cool the burning surface. As the nozzles continue to spray, more water mist droplets penetrate through the fire plume, significantly cool the fire plume, and affect the chemical reaction rate inside the plume. Finally, the temperature of fire plume is decreased to be low enough that the fire is extinguished. The fire suppression time decreases as the increasing water mist flow rate injection. The higher injection flow rates will result in the higher momentum of water mist droplets and consequently cause more droplets to penetrate into the fire plume. Figure 12 show the temperature and gas concentration of two different nozzle flow rate (5 and 25 L/min), the fire extinguishment time for high flow rate is

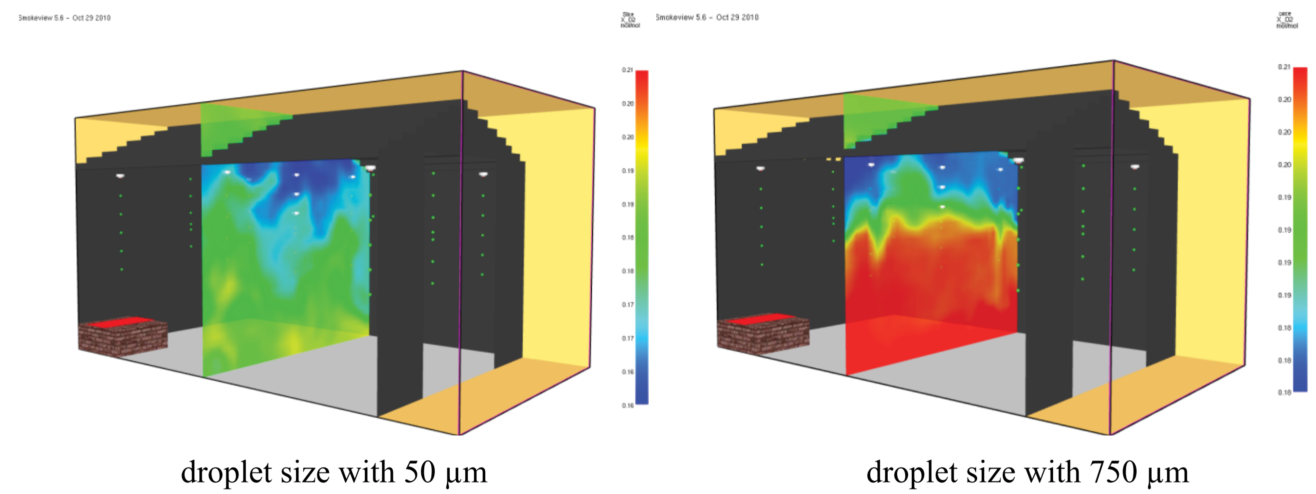

Figure 5: Oxygen contours at the center of hanger.

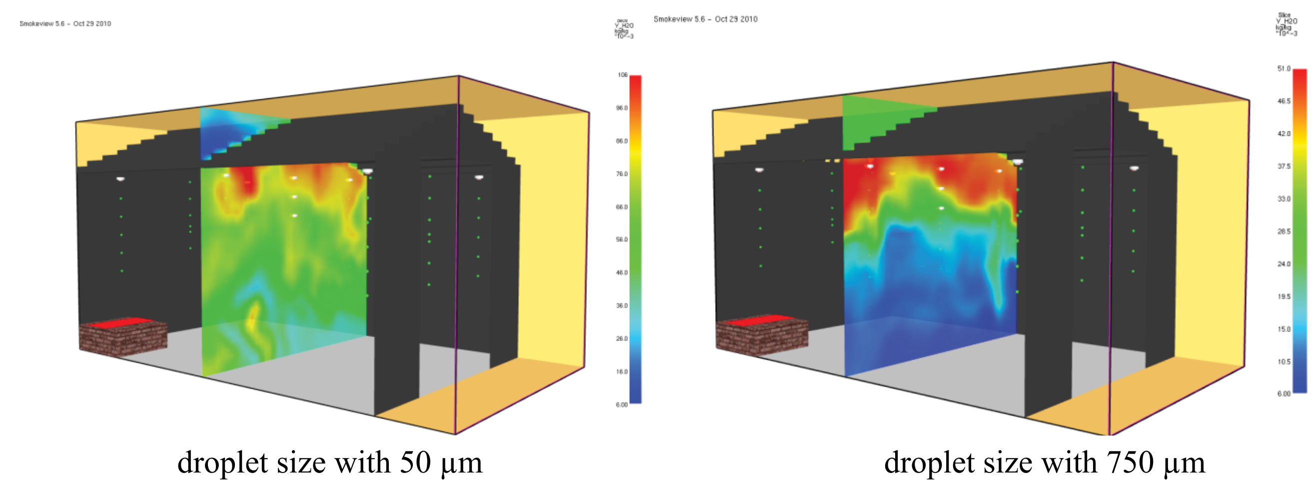

Figure 6: Steam contours at the center of hanger.

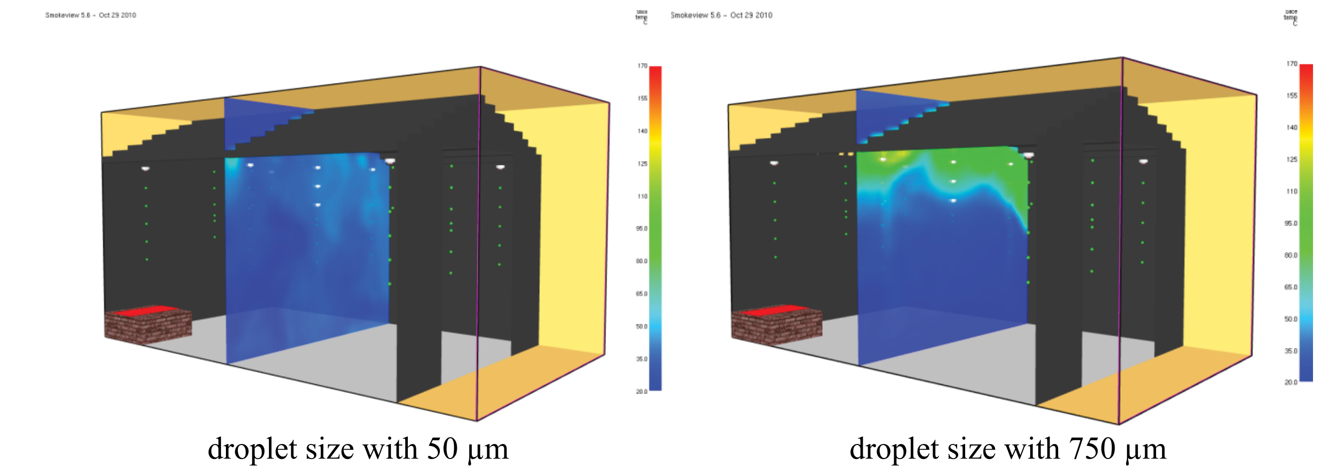

Figure 7: Temperature contours at the center of hanger.

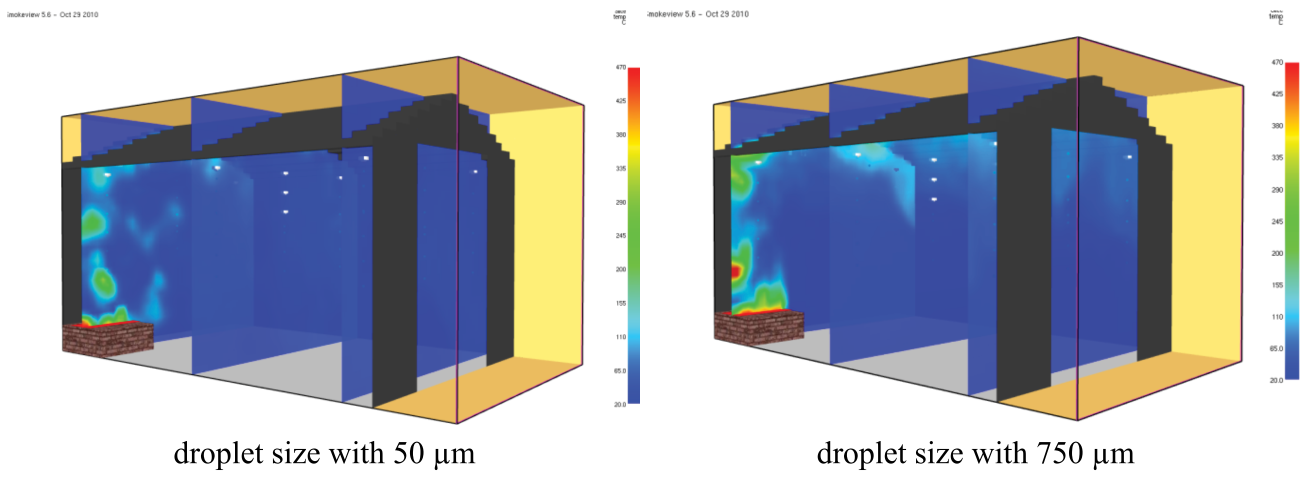

Figure 8: Temperature contours at different locations of hanger.

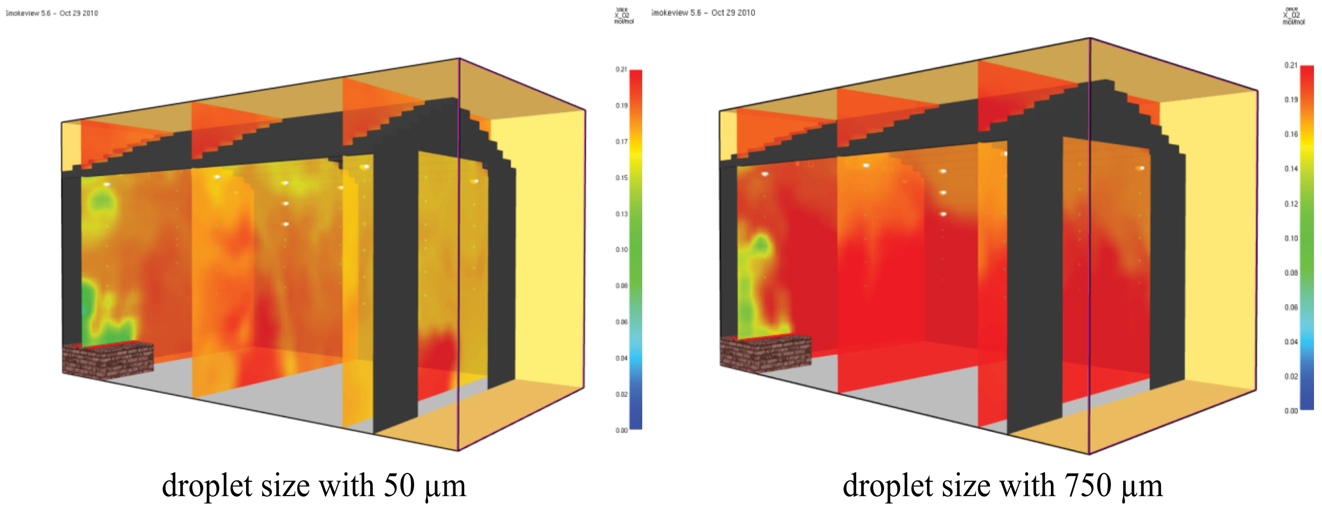

Figure 9: Oxygen contours at different locations of hanger.

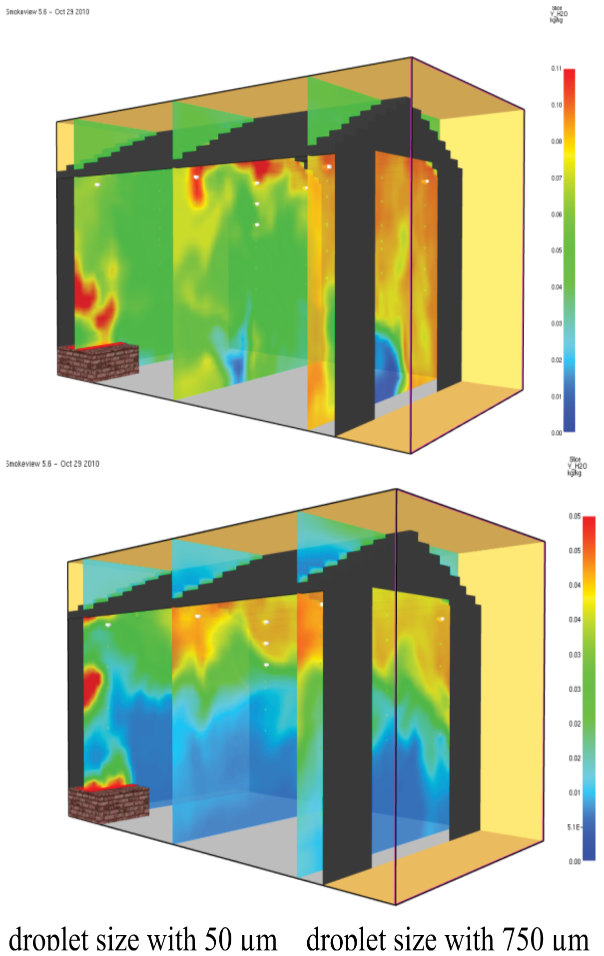

Figure 10: Steam contours at different locations of hanger.

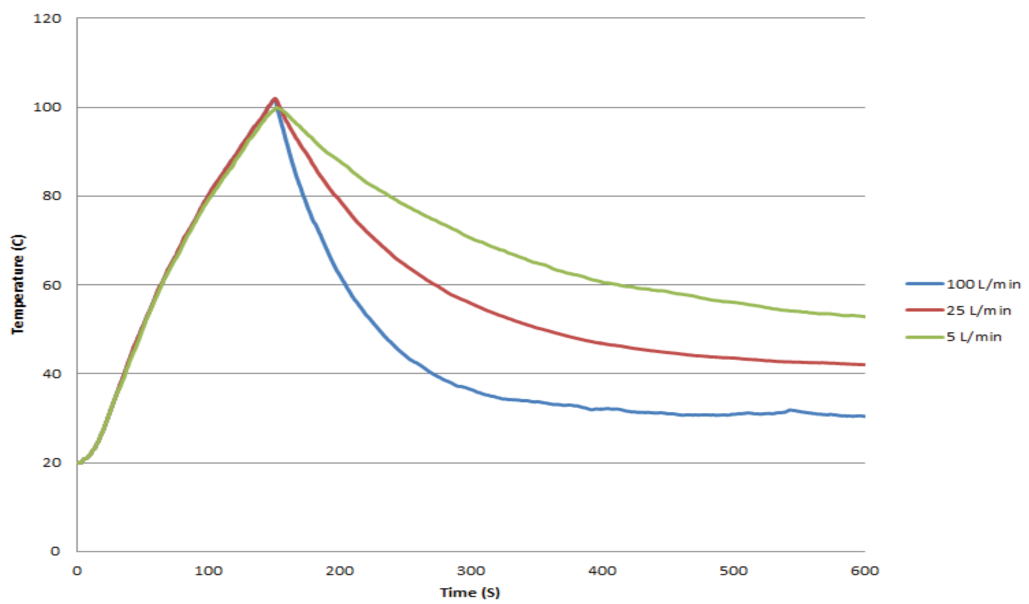

Figure 11: Average temperatures with different nozzle flow rate.

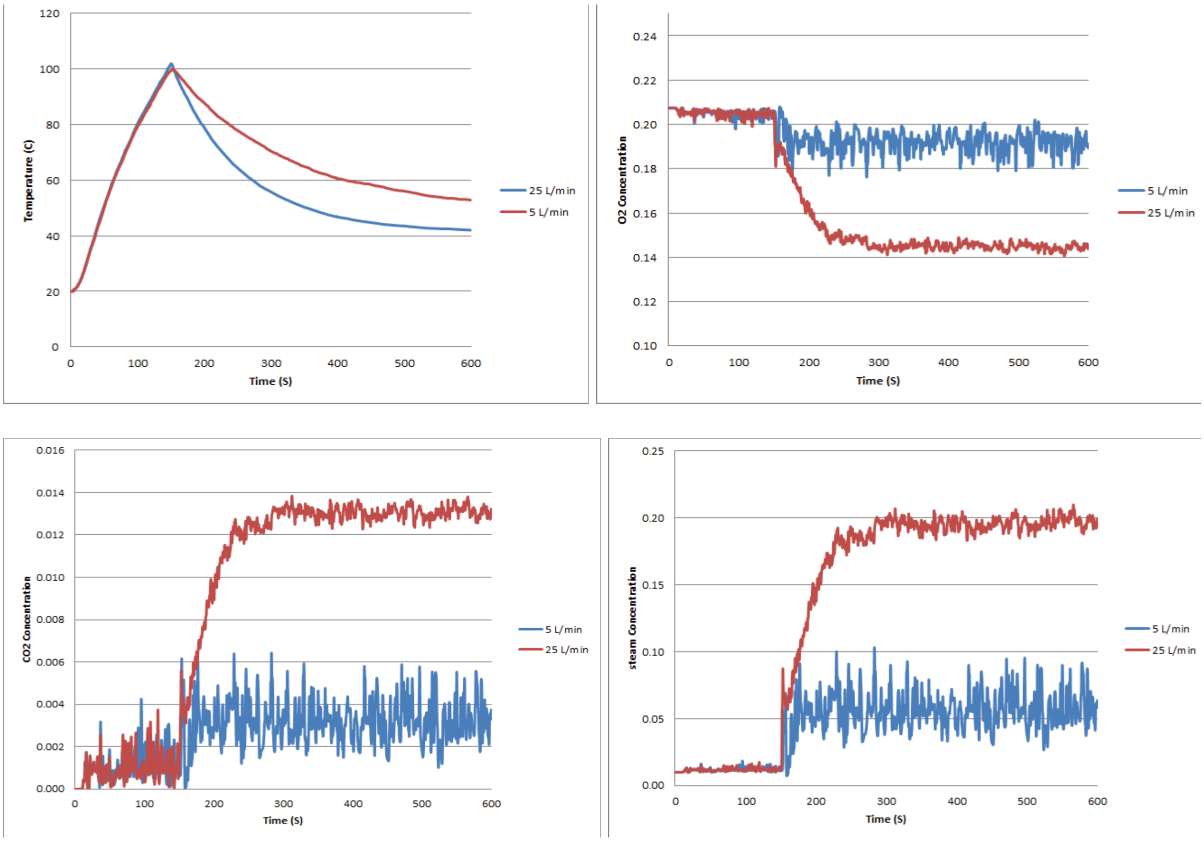

Figure 12: Temperature and gas concentration with flow rate (5 and 25 L/min).

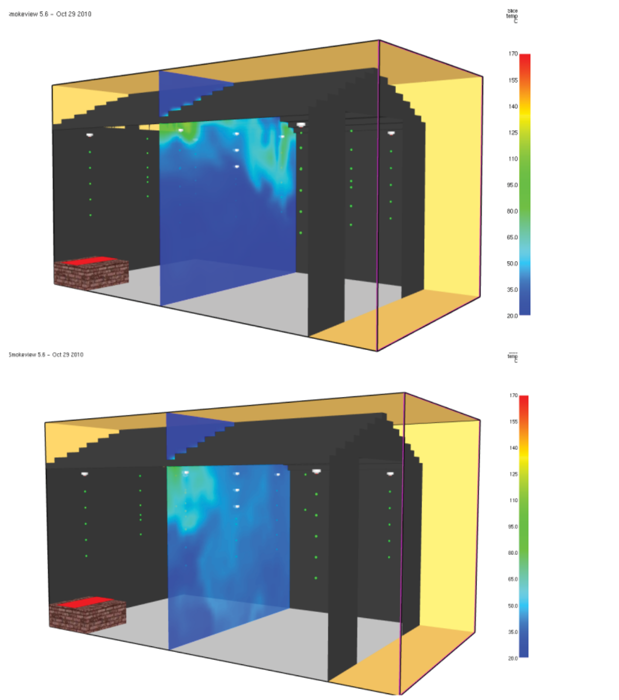

Nozzle flow rate (5 L/min) Nozzle flow rate (25 L/min)

Figure 13: Temperature contours at the center of hanger.

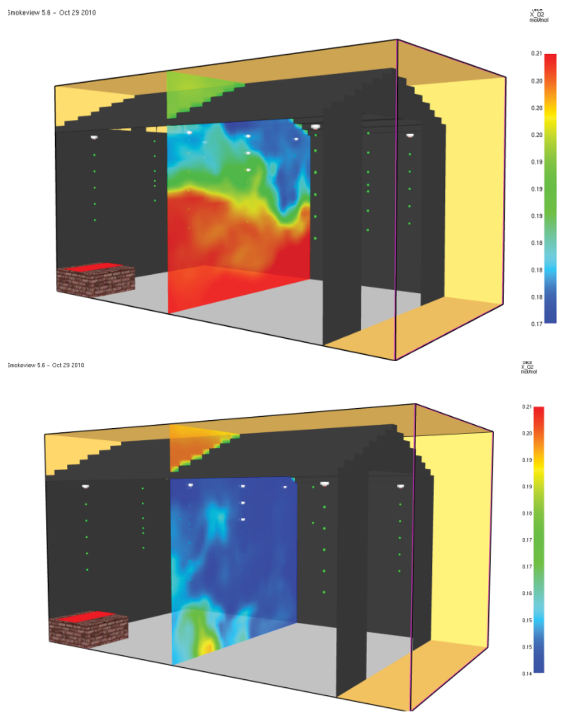

Nozzle flow rate (5 L/min) Nozzle flow rate (25 L/min)

Figure 14: Oxygen contours at the center of hanger.

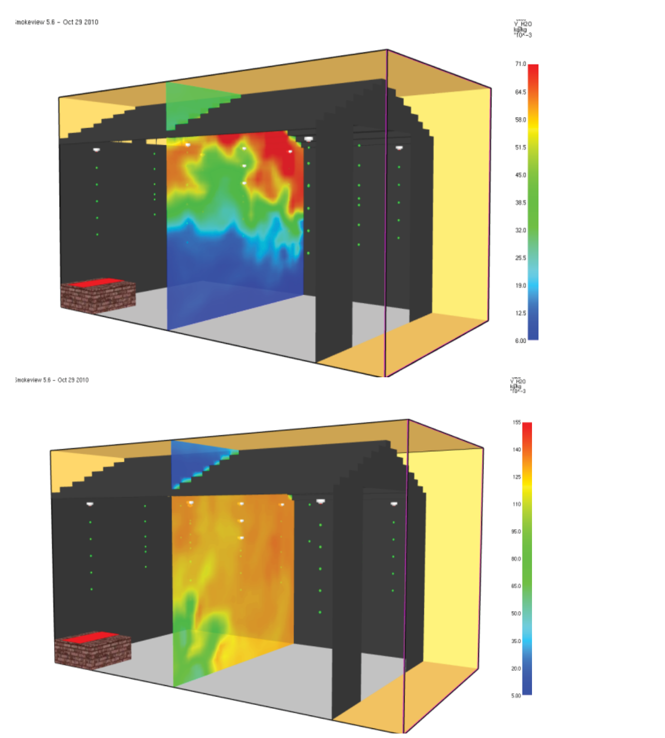

Figure 15: Steam contours at the center of hanger.

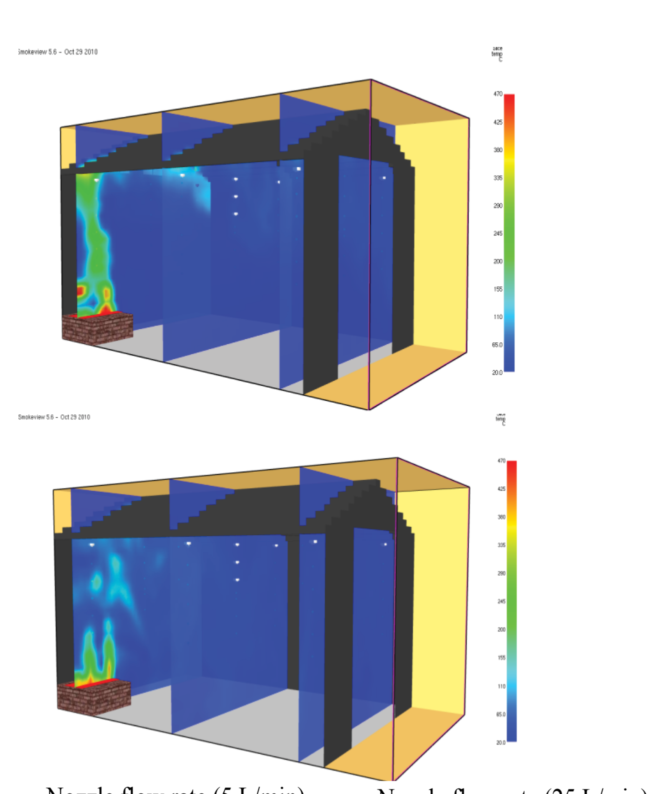

Figure 16: Temperature contours at different locations of hanger.

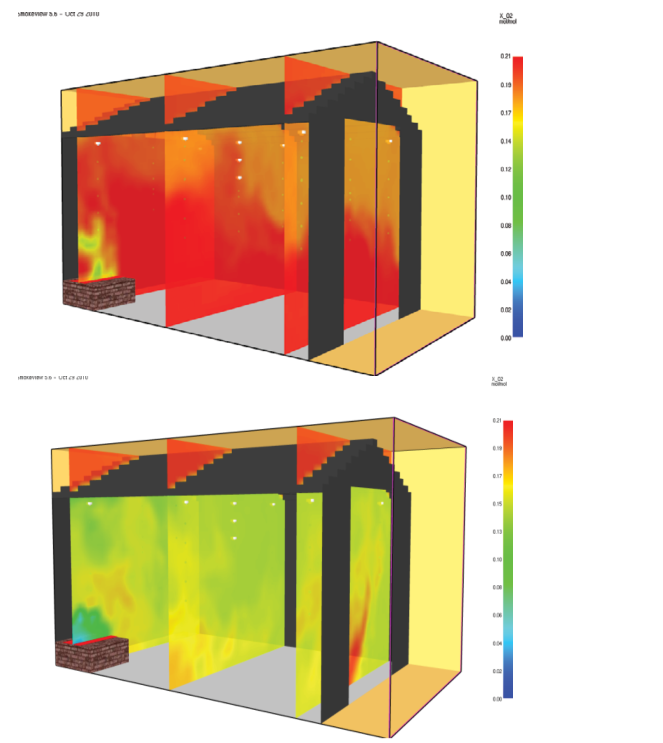

Figure 17: Oxygen contours at different locations of hanger.

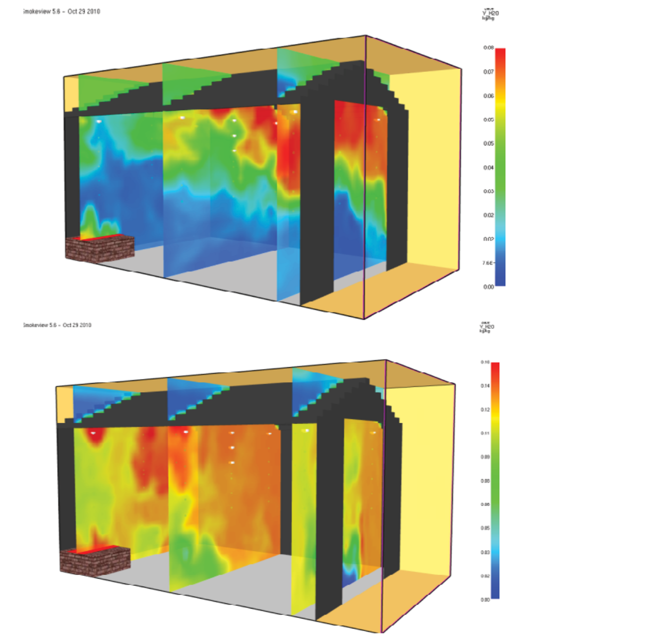

Figure 18: Steam contours at different locations of hanger.

decrease as small flow rate increase as discussed before. Also the O_2 concentration of small flow rate (5 L/min) is increase by comparison with high flow rate (25 L/min) decrease. CO_2 and steam concentration are increase for high flow rate. Figures 13-18 shows the temperature, O_2 and steam concentration contours for two flow rate of nozzle (5 and 25 L/min) at the center and different locations inside hanger.

Conclusion

In this paper, the effect of various droplet sizes of water mist and nozzle flow rate on fire spread in hanger are studied by numerical simulations using the FDS. From the previous results we arrive at the following major conclusions:

1. The fire extinguishing time increased with the droplet size, and decreased with the increase in the nozzle flow rate.

2. The gas concentrations were directly affected by fire extinguishing time. With the increase in time, the oxygen value decreased, while the water vapour and carbon dioxide increased.

3. Temperature decay rates increase with the decrease of droplet size for the same flow rate.

4. Temperature decay rates increase with the increase of nozzle flow rate.

References

1. Factory Mutual (2000) The Facts About Water Mist Systems. Approved Product News 16: 2.
2. Ananth R, Ndubizu CC, Tatem PA (2000) The Effects of Droplet Size and Injection Orientation on Water Mist Suppression of Low and High Boiling Point Liquid Pool Fires, Combustion Science and Technology, Vol. 157,Gordan and Breach Science Publishers Imprint, Malaysia, pp: 63-86.
3. Liu Y, Jiang Z, Wang D, Li X (2014) Experimental research on the water mist fire suppression performance in an enclosed space by changing the characteristics of nozzles, Research Center of Hydraulic and Pneumatic Technology, School of Mechanical Science and Engineering, Huazhong University of Science and Technology, Wuhan, Hubei 430074.
4. Sung CK, Hong SR (2003) The Effect of Water Mist on Burning Rates of Pool Fire, J Fire Sci 4: 305-323.
5. Hume BP (2003) Water Mist Suppression in Conjunction with Displacement Ventilation. School of Engineering, University of Canterbury Private Bag 4800 Christchurch, New Zealand.
6. Back GG III, Beyler CL, Hansen R (2000) A quasi-steady-state model for predicting fire suppression in spaces protected by water mist systems. Fire Safety J 35: 327-362.
7. Kumar K, Khoo BC, Xue H, Hua J (2002) A numerical study of the interaction of water spray with a fire plume. Fire Safety J 37: 631-657.
8. http://fdssmv.googlecode.com/svn/trunk/fds/trunk/manuals/all_PDF_files/FDS_5_technical_reference_guide.PDF.
9. Anderson DA, Tannehill JC, Pletcher RH (1984) Computational Fluid Mechanics and Heat Transfer. Hemisphere publishing Corporation, Philadelphia, Pennsylvania 11: 15.
10. McGrattan KB, Hostikka S, Floyd JE, Baum HR, Rehm RG (2007) Fire Dynamics Simulator (Version 5), Technical Reference Guide. NIST Special Publication 10185, National Institute of Standards and Technology, Gaithersburg, Maryland.
11. Shalaby H, Kohl KJ, Grabski R (2009) Interaction of water mist with fire plume by using FDS. Jahresbericht 2006/2007/2008, IdF Sachsen-Anhalt, Heyrothsberge.
12. Incropera FP, De Witt DP (1996) Fundamentals of Heat and Mass Transfer. John Wiley and Sons, New York, (4thedn).
13. Ranz WE, Marshall WR (1952) Evaporation from drops: part II. Chemical Engineering Progress 48: 173-180.
14. Mawhinney JR, Richardson JK (1996) A Review of Water Mist Fire Suppression Research and Development. Technical Note, Fire Technology First Quarter pp: 54-89.